# The Role of the Spatial and Temporal Radiation Deposition in Inertial Fusion Chambers: The case of HiPER

J. Alvarez 1), D. Garoz 1), R. Gonzalez-Arrabal 1), A. Rivera 1), M. Perlado 1)

1) Instituto de Fusión Nuclear, UPM, Madrid (Spain)

E-mail contact of main author: jalvarezruiz@yahoo.com

**Abstract.** The first wall armor for the reactor chamber of HiPER will have to face short energy pulses of 5 to 20 MJ mostly in form of X-rays and charged particles at a repetition rate of 5-10 Hz. Armor material and chamber dimensions have to be chosen to avoid/minimize damage on the chamber, assuring the proper functioning of the facility during its planned lifetime. The maximum energy fluence which the armor can withstand without risk of failure will come determined by how radiation deposits its energy in time and space in the material. In this paper, simulations on the thermal effect of the radiation-armor interaction are carried out with an increasing definition of the temporal and spatial deposition of energy to prove this critical point. These calculations will lead us to present the first simulated values of the thermo-mechanical behavior of the tungsten armor designed for the HiPER project under a shock ignition target of 48 MJ. The results will show that only the crossing of the plasticity limit in the first few microns might be a threat after thousand of shots for the survivability of the armor.

## 1. Introduction

Fusion reactions in inertial confinement devices are characterized by short (some ns long) and very energetic explosions (from some tens to some hundred of MJ) which yield neutrons, gamma and X rays and high energy ions. Among those products, neutrons account for around 70% of the fusion energy and show almost no interaction with the first wall of the reaction chamber. If no protection scheme is devised (ion deflector or a high Z gas), the remaining 30% of the energy in the form of X-rays and ions is deposited on the inner wall of the chamber and the front-end optics. Thus, dry-wall designs rely on large chamber dimensions (usually 5-6 m in radius) and an inner wall armor to typically withstand heat loads of 1-6 J/cm$^2$ and powers of some GW/m$^2$. From the thermo-mechanical point of view, this armor has to be made of a material with a high thermal conductivity and melting/sublimation point and with good properties to mechanical stress and fatigue. The goal is to avoid or at least to minimize the mass loss and cracking leading to mechanical failure. The materials under consideration for that purpose are tungsten and carbon based composites. However, nowadays, the tritium retention problem of carbon compounds makes tungsten the standard option on most armor designs [1]. A look at the bibliography shows that, the now canceled American HAPL project [2] relied on a tungsten armor for the 7.5 m radius chamber to absorb the energy from 150 MJ targets (average wall load 5.5 J/cm$^2$) at a 5-10 Hz repetition rate. The Japanese Falcon D design [3] also considered tungsten as the most adequate armor material for the reaction chamber. In their design, they planned a 5-6 m radius chamber to house 40 MJ (an average wall load of 2 J/cm$^2$) fusion targets at a repetition rate of 30 Hz. The European inertial fusion project, HiPER [4], is meant to use targets of intermediate energies (some tens of MJ up to 100 MJ maximum) at a repetition rate of 5 to 10 Hz. For an initially planned chamber of 5 m radius and a 50 MJ target, tungsten will have to accommodate heats load of around 4 J/cm$^2$ per shot.

This paper presents the first simulation numbers for the HiPER project on the thermo-mechanical behavior of tungsten armor for the proposed 5 m radius chamber under the explosion of a shock ignition target of 48 MJ. First, the characterization of the products of a shock ignition target are described. Then, a series of simulations is presented to highlight the importance of a proper modeling of the time profile of the delivered energy and its spatial deposition. Finally, the resulting thermo-mechanical behavior of the tungsten armor when the spatial and temporal profile of the energy deposition is accurately accounted for is shown. Some final conclusions based on the simulation results are discussed.

## 2. Fusion products of a shock ignition target

Fusion targets are filled with deuterium and tritium which, when compressed and ignited, generate 14.1 MeV neutrons and 3.5 MeV He ions. Through different processes, that energy is redistributed among the non-burnt ions (D and T and atoms from the target plastic cover, typically C and H) and in form of X-rays. To study the thermo-mechanical effects of the chamber armor against this radiation, the total amount of energy deposited on the wall is not sufficient. As it is shown later, it is necessary to accurately know the distribution and energy spectra of the different products which be calculated using a radiation-hydrodynamic code.
One of the goals of the HiPER project is to reduce the required laser energy to achieve fusion compared to current approaches (for example, NIF [5]). Thus, HiPER is initially opting for Fast or Shock ignition targets which, in principle, requite around 1/3 of the energy of the central ignition targets. For the studies presented in this work, we have chosen the product spectra of a 48 MJ shock ignition target obtained using the LASNEX code [6,7]. In table 1, the energy distribution among the different species is summarized and one can already identify the most relevant particles in the plasma-armor interaction. Since neutrons do not interact with the armor, deuterium, tritium and helium are the main species responsible for the delivery of energy on the armor. Carbon atoms are the next species but their contribution to the total deposition of energy on the wall will be obviated in the thermo-mechanical study. (Carbon content and its energy spectra is very dependent on the target design and its inclusion would influence the validity of the results for a general case). X-rays deliver only a 1.4% of the fusion energy to the armor but, as it will be shown, they play an important role in the simulations due to their prompt deposition of energy and consequently high power load on the walls. Other species such as gamma rays, protons and isotopes will be excluded for their minor effect.

TABLE 1. ENERGY DISTRIBUTION OF A 48 MJ SHOCK IGNITION TARGET

| | Energy (J) Total= $48\times10^6$ | % |
|---|---|---|
| X-rays | $6.8\times10^5$ | 1.42% |
| Neutrons | $3.6\times10^7$ | 75.03% |
| Deuterons | $2.9\times10^6$ | 6.04% |
| Tritons | $3.5\times10^6$ | 7,29% |
| He | $3.6\times10^6$ | 7.5% |
| C | $1\times10^6$ | 2,08% |
| Gamma rays H, $^3$He, $^{13}$C | $3\times10^5$ | 0.63% |

Thus, figure 1 shows a detailed description of the distribution and energy spectra of the relevant particles to our thermo-mechanical study of the armor. D,T, He and X-rays deliver in total a energy of 10.7 MJ to the wall.

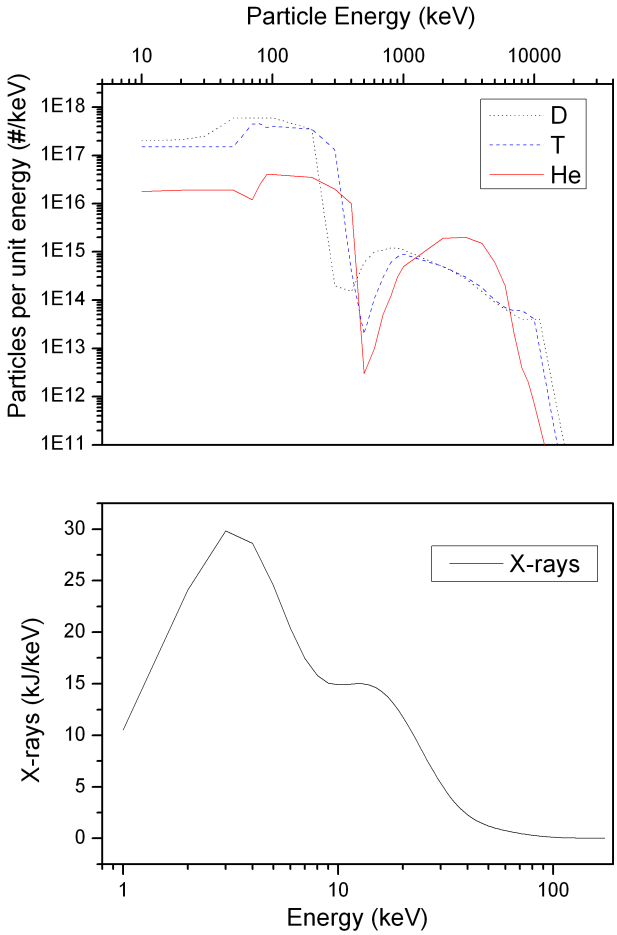


*FIG. 1.(Upper) Energy spectra of D,T and He, and (lower) X-rays of a 48 MJ shock ignition target.*

As it will be shown later, the characterization of the temporal profile of energy deposition is required for a proper simulation of the thermo-mechanical study of the armor. In the case of ions, this temporal profile can be calculated from their kinetic energy spectra of figure 1. Considering a reaction chamber of 5 m in radius, the arrival time of D, T and He particles is represented in figure 2. In the case of the X-rays in which all photons travel at the same speed, the temporal profile comes determined by the time span in which they were created. According to previous calculations, the X-ray pulse duration has been estimated to be around 1 ns [8].

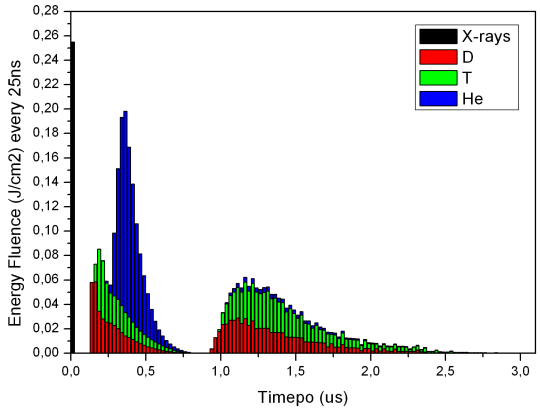


*FIG. 2. Temporal profile of the energy deposition of X-rays, He, D and T on a 5 m radius chamber for a 48 MJ shock ignition target. Histograms correspond to time intervals of 25 ns. Bars of the different species are added up to show the total energy deposition on each time step.*

Figure 2 shows how the different species contribute to the deposition of energy in time steps of 25 ns for a 5 m radius chamber. As it can be seen, X-rays arrive almost immediately after the ignition, depositing their energy (6.3% of the 10.7 MJ) at around 17 ns. Then, the fast D, T and He involved in the ignition arrive at around 150 ns after the explosion. Those fast particles have deposited their energy (50% of the 10.7MJ) in the armor before the first μs. Finally, slow D and T particles and thermal He arrive to the armor after the first μs and deposited their energy (the remaining 44%) during 1.5 μs. In around 2 μs, all the fusion energy which will be delivered to the armor, 10.7 MJ, is deposited.

Finally, the spatial deposition of that energy in the armor is also relevant for an accurate simulation of the thermo-mechanical behavior of the armor. The spatial energy profile of the different ions can be calculated using the SRIM code [9]. Considering tungsten as the armor material, SRIM simulations are presented in figure 3. In the case of X-rays, the spatial deposition has been estimated using the absorption coefficient tables [10] of X-ray on W in our spectral region of interest (figure 2). It is important to notice that more than 50% of the total energy is deposited just in the first micron. In the first two microns around 66% of the energy is deposited. This implies that all energy deposited at higher depths (as is the case of fast D and T ions which penetrate some hundred microns, or energetic X-rays which travel some tens of microns) will play very little role in the thermo-mechanical behavior of W. A rough estimate indicates that around 15 to 20% of the arriving energy will be deposited in the W armor with almost no thermo-mechanical effect.

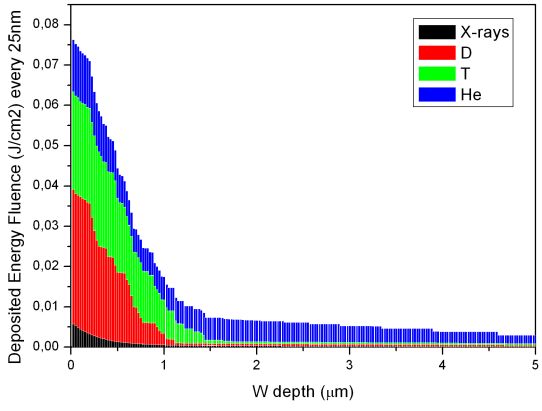

*FIG. 3. Spatial distribution of the deposited energy for the indicated particles.*

## 3. Simulations and results

In principle, HiPER has been proposed as a spherical chamber of 10 m in diameter with a 1 mm tungsten armor as inner wall. In order to simulate the thermal effects on the armor due to its exposure to radiation, we consider three different scenarios:
Scenario 1 – Energy is deposited on the surface during some μs continuously.
Scenario 2 – Energy is deposited on the surface following the real temporal distribution.
Scenario 3 – Energy is deposited taking into account the penetration depth of the different particles and the real temporal profile.

This exercise will show the importance of an accurate description of the spatial and temporal deposition of energy in the case of simulations for inertial fusion. The heat load on plasma facing materials takes place in such short pulses and with such broad energy spectra of species that approximations as the ones used in magnetic confinement fusion (constant deposition of energy in the first micron of the material) are not valid. Thus, parameters as the Heat Flux value [11] and the roughening and melting limits for tungsten should be handled with care.

The calculations have been carried out using the multi-physics open software CODE ASTER [12]. This software allows to vary the physical and mechanical constants as a function of temperature which has been implemented for our calculations using the ITER material handbook [13]. In all cases and for simulation purposes, the 1 mm W armor is in contact with a fictitious coolant at a constant temperature of 600 K. Also note that in these simulations, no other effect but the deposition of energy in the first wall is considered. Thus, atomistic effects such as sputtering, production of defects and changes in the chemical composition of the armor are not taken into account.

### 3.1 – Scenario 1 – Energy is deposited on the surface during some us continuously.

The simplest scenario possible in the deposition of energy on the armor is to consider that all the radiation energy is deposited evenly in time on the surface. Thus, for our case, the total amount of energy delivered by the X-rays, D, T and He ions is 10.7 MJ, which corresponds to an energy fluence of 3.4 J/cm2 for a 5 m radius chamber. This energy can be considered as deposited in a time of 2 μs (see figure 2). This one-dimensional heat equation problem has analytical solution and yields a maximum temperature value on the surface of 1900 K. Taking into account the temperature dependence of the physical properties of W, the simulation was performed using the CODE ASTER software. Figure 4a shows how temperature reaches a maximum of 2200 K at the end of the pulse. After the 2 μs, the temperature decreases rapidly due to the high thermal conductivity of W (173 W/m/K), reaching the base temperature of 600 K after 10 ms. Without further discussion, we can say that, since W can displace heat so quick, the fact that the time profile of the deposition of energy is not considered will give us an underestimation of the maximum temperature.

### 3.2 -Scenario 2 -Energy is deposited on the surface following the real temporal distribution.

The first refinement in our simulations to be considered is to include a proper temporal profile of the energy deposition on the W armor. As expected, simulations (figure 4b) yield quite different results from that of the scenario 1. The first evident conclusion is that the

temperature evolution of the armor follows the time structure of the radiation pulse, reaching at certain points higher temperatures and dropping to the base temperature after some ms. The most remarkable results is that, according to the simulations, the fast energy delivery of the X-ray pulse leads to temperatures above the melting point (3600 K). However, experiments with X-ray sources have shown that W stars to melt at much higher energy fluences [14]. This time, one must realize that the deposition of energy only on the surface obviates the fact that the radiation energy has a spatial profile inside the W according to the penetration depth of the different particles. This simplification in the modeling leads to an overestimation of the maximum temperatures.

### 3.3 - Scenario 3 – Energy is deposition taking into account the penetration depth of the different particles and the real temporal profile.

In this scenario, we consider the temporal and spatial profile of the energy deposition of the radiation in the W armor. A detailed description of the temporal and spatial distribution of energy differs from previous scenarios (figure 4c). The temperature evolution at different depths clearly shows similar results to those obtained for other W armors [2] and the highest temperature does not reach 1800 K. Once again, the W armor diffuses away all heat before the next pulse.

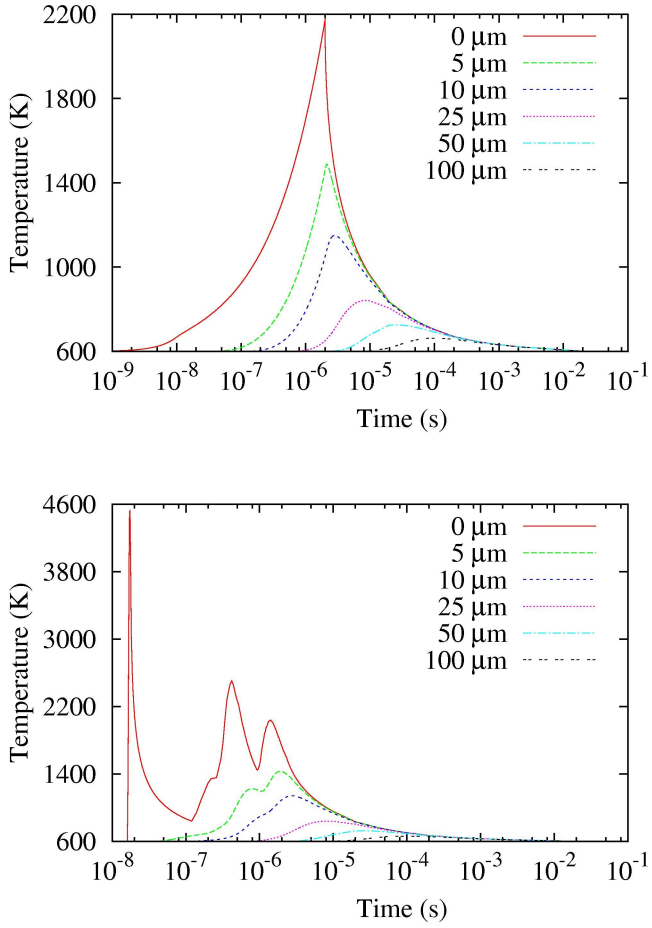

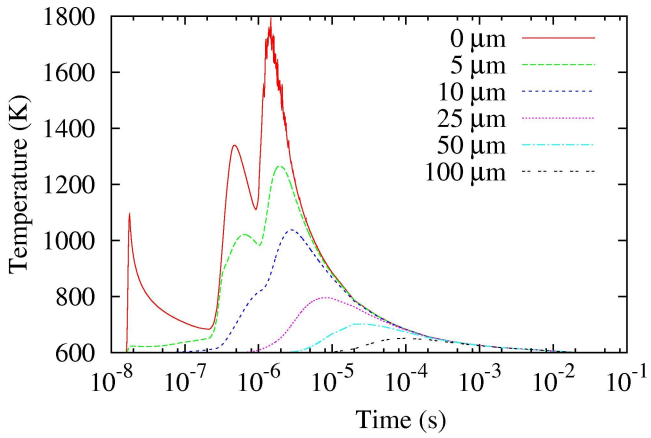


*FIG. 4. Temperature evolution at different tungsten depths for a heat load of 3.4 J/cm² under a) scenario 1(upper) , b) scenario 2 (mid) and c) scenario 3 (lower).*

Under these proper conditions for the deposition of energy, we also carried out a 2D analysis on the mechanical behavior of the W armor with CODE ASTER. The observed increase of temperature generates a measurable expansion of the W which, in turn, causes compressions in the wall. The main compression is tangent to the surface of the wall because W only can expand in radial direction due to geometrical considerations. Figure 5 shows temperature and Von Misses stress ($\sigma_{VM}$), which measure the stress compression into the wall, as function of the depth at a fixed time of 1.5 µs. When temperature increases, the expansion of the material produces an increase in the stress. The presented stress has been obtained considering the hypothesis that tungsten behaves as an elastic material, so when the Von Misses stress is higher than the Yield Strength (also represented in figure 5), the tungsten suffers plastic strain. The fact that at high temperature the Yield Strength decreases makes that crossing more favourable. Thus, plastic strain is located in the first microns of the wall, reaching around 18 µm in times after 1.5 µs. When the temperature decreases and W returns to its initial volume, there are residual traction stress in this layer. As detailed by Blanchard and Martin [15], fatigue due to cycle plastic strain might produce cracks at the surface. The possibility that these cracks, together with other atomistic effects, influence on the survivability of the W armor with increasing fusion shots is under debate [15].

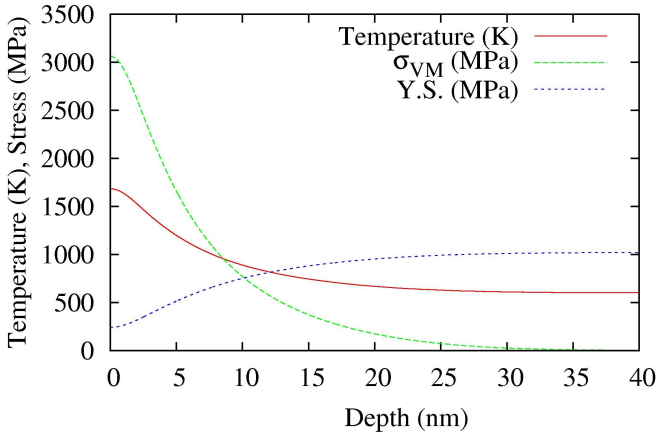


*FIG. 5 – Temperature, Von Misses stress and Yield Strength as function of depth at 1.5 µs,of simulation.*

## Conclusions

The inner wall of an inertial fusion reaction chamber will have to withstand high power loads five to ten times a second. With no ion or X-ray protection, only relative large chambers (5-8 m radius) and wall armors made of high resistant materials to thermal loads and mechanical stresses (as tungsten) can handle this harsh environments. In order to appropriately study the thermo-mechanical effects of the fusion radiation on the armor , one has to fully account for the precise temporal and spatial deposition of the radiation on the material. Avoiding to do that will underestimate or overestimate the energy fluence limit ($J/cm^2$) to preserve the lifetime of the armor. This point has been clearly demonstrated on these pages.
Moreover, this work shows the first thermo-mechanical studies on the W armor for the HiPER project under the radiation of a 50 MJ shock ignition target. Calculations reveal that, W armor will work well below its melting point. Only mechanical effects due to transitions of W to its plasticity phase could affect its performance. Fatigue and eventually crack formation under hundred/thousand fusion shots might end in mass loss and irreversible damage.

## References

[1] M. Kaufmann, R. Neu. Fusion Engineering and Desing 82 (2007) 521
[2] A.R. Raffray, J. Blanchard, J. Latkowski, F. Najmabadi, T. Renk, J. Sethian, S. Sharafat, L. Snead, Fusion Engineering and Design 81 (2006) 1627
[3] T. Goto, Y.Someya, Y. Ogawa, R. Hiwatari, Y. Asaoka, K. Okano, A. Sunahara, T. Johzaki, Nucl. Fusion 49 (2009) 075006,
[4] **http://www.hiper-laser.org/**
[5] E. I. Moses. Energy Conversion and Management 49 (2008) 1795
[6] G. Zimmerman et al., Journal of the Optical Society of America 68 (1975) 549
[7] J. Perkins. Internal report
[8] J. Perkins. Internal report (see presentation: **http://www.docstoc.com/docs/54806737/Temperature-Response-and-Ion-Deposition-in-the-1-mm** )
[9] **http://www.srim.org/**
[10] **http://www.nist.gov/physlab/data/xraycoef/index.cfm**
[11] J. Linke et al. J. Nucl. Mater. 367-370 (2007) 1422 .
[12] **http://www.code-aster.org/**
[13] Tungsten properties ITER Material Handbook **http://aries.ucsd.edu**
[14] T. J. Tanaka et al. J. Nucl. Mater. 347 (2005) 244 .
[15] J.P. Blanchard and C.J. Martin. J. Nucl. Mater. 347 (2005) 192